PAN ARCHIVES OF ACOUSTICS
Vol. 40, No. 2, pp. 223–234 (2015)

DOI: 10.1515/aoa-2015-0025

Sound Radiation from a Surface Source Located at the Bottom of the Wedge Region

Krzysztof SZEMELA

Department of Mechatronics and Control Science
Faculty of Mathematics and Natural Sciences
University of Rzeszów
Prof. St. Pigonia 1, 35-310 Rzeszów, Poland; e-mail: alpha@ur.edu.pl

(*received December 12, 2014; accepted March 20, 2015*)

Applying rigorous analytical methods, formulas describing the sound radiation have been obtained for the wedge region bounded by two transverse baffles with a common edge and bottom. It has been assumed that the surface sound source is located at the bottom. The presented formulas can be used to calculate the sound pressure and power inside the wedge region. They are valid for any value of the wedge angle and represent a generalization of the formulas describing the sound radiation inside the two and three-wall corner region. Moreover, the presented formulas can be easily adapted for any case when more than one sound source is located at the bottom. To demonstrate their practical application, the distribution of the sound pressure modulus and the sound power have been analyzed in the case of a rectangular piston located at the wedge's bottom. The influence of the transverse baffle on the sound power has been investigated. Based on the obtained formulas, the behaviour of acoustic fields inside a wedge can be predicted.

Keywords: wedge region, sound pressure, sound power, Neumann boundary value problem, Helmholtz equation, vibrating piston, Hankel transform.

1. Introduction

Theoretical analysis of sound radiation allows noise reduction in the human environment to be performed in an efficient way. Some vibrating surfaces, which can be easily found as components of machines, vehicles, or architectural structures, represent surface sound sources. Therefore, active noise control as well as theoretical investigations are of considerable importance in the case of such sound sources. The methods based on the use of piezoelectric elements and various algorithms have been proposed to reduce the vibrations of structures (Górski, Morzyński, 2013; Leniowska, 2009; Mazur, Pawełczyk, 2013; Wiciak, Trojanowski, 2013). Acoustic behaviour of vibrating surfaces can be predicted on the basis of theoretical investigations. This means that the acoustic properties of a considered vibroacoustic system can be optimized at the stage of construction, which allows application of effective noise control. The sound radiation of some baffled surface sources has been analyzed by use of some advance methods (González-Montenegro *et al.*, 2014; Palumbo, 2009). At present, modern architectural structures consist of some walls with different shapes and acoustic properties. The buildings' walls can be arranged in a different way, leading to the popularity in urban areas of such spatial regions as, for example, the two-wall corner, three-wall corner, wedge, cylinder. Therefore, it is of interest to analyze the sound radiation inside the spatial regions of different shapes. The Green's function for the two-wall corner region and three-wall corner region has been obtained (Rdzanek, Rdzanek, 2006). Then, the sound radiation of surface sources located at the boundary of the two-wall corner and three-wall corner region has been investigated (Rdzanek *et al.*, 2007; Szemela, 2014; Szemela *et al.*, 2012). Moreover, the acoustic behaviour of a spherical sound source inside a quarterspace has been analyzed (Hasheminejad, Azarpeyvand, 2004). The acoustic properties of rectangular rooms have also been discussed (Aretz *et al.*, 2014; Godinho *et al.*, 2011; Meissner, 2013). Acoustic waves propagated in wedges have been analyzed by use of various methods (Abawi, Porter, 2007;

Budaev, Bogy, 2003; Hladky-Hennion *et al.*, 1998). The acoustic behaviour of the wedge room has been discussed as well (Mechel, 2013).

So far, the formulas describing the sound radiation of a surface source located at the bottom of the wedge region are unknown. Therefore, the main aim of this study is to obtain the rigorous analytical formulations determining the sound pressure and sound power in the case of the wedge region with the perfectly rigid infinite transverse baffles and bottom, and an arbitrary wedge angle. They will represent a generalization of the formulas valid for the two- and three-wall corner regions which can be obtained based on the presented in the literature Green's functions.

2. Statement of the problem

The sound radiation has been analyzed inside the wedge region. It has been assumed that the considered region is bounded by two flat infinite transverse baffles with a common edge and bottom which is aflat infinite baffle. The wedge's transverse baffles and its bottom are perfectly rigid. It is necessary to emphasize that the considered model of the wedge region can be used only to describe the sound radiation in the case when the wedge's walls are nearly rigid and their dimensions are much greater than the acoustic wavelength. The transverse baffles are perpendicular to the bottom. The angle between the wedge's transverse baffles φ_0, called the wedge angle, can vary within the limits of $0 < \varphi_0 \leq 2\pi$. It can be noticed that for $\varphi_0 = \pi/2$ and $\varphi_0 = \pi$, the wedge region is the three- and two-wall corner regions, respectively. The field point's location is described in the cylindrical coordinate system by the vector $\mathbf{r} = (r, \varphi, z)$. The sound source is located at the bottom of the wedge region, i.e., on the plane $z = 0$. Additionally, to determine the sound source's location, the Cartesian coordinate system (x, y) has been introduced on the plane $z = 0$. The considered region with a sound source and the introduced Cartesian coordinate system has been illustrated in Fig. 1.

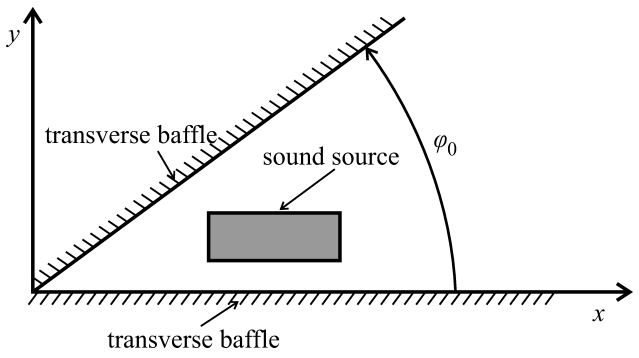

Fig. 1. Wedge region with a sound source located at the bottom. The introduced Cartesian coordinate system and the wedge angle φ_0 between the wedge's transverse baffles.

The medium inside the region is lossless, homogeneous, and isotropic. The amplitude of acoustic waves is small enough to use the acoustic field linear theory. All the analyzed processes have been considered as steady-state and time-harmonic. On the basis of the introduced assumptions, the acoustic potential $\Phi(\mathbf{r})$ can be found as the solution of the Helmholtz equation given by (cf. Crocker, 2010)

$$\Delta\Phi(\mathbf{r}) + k^2\Phi(\mathbf{r}) = 0, \tag{1}$$

where $\Delta = \partial^2/\partial r^2 + (1/r)\,\partial/\partial r + (1/r^2)\partial^2/\partial\varphi^2 + \partial^2/\partial\, z^2$ is the Laplacian in the cylindrical coordinates, $k = \omega/c$ is the wavenumber, $\omega = 2\pi f$ is the angular frequency, f is the vibration frequency, and c is the sound speed in the medium. In the case of the considered wedge region, the following boundary condition can be imposed:

$$\left.\frac{\partial\Phi(\mathbf{r})}{\partial\varphi}\right|_{\varphi=0} = \left.\frac{\partial\Phi(\mathbf{r})}{\partial\varphi}\right|_{\varphi=\varphi_0} = 0, \tag{2}$$

$$\left.\frac{\partial\Phi(\mathbf{r})}{\partial z}\right|_{z=0} = -v(r,\varphi), \tag{3}$$

where

$$v(r,\varphi) = \begin{cases} v_S(r,\varphi), & \text{on the surface } S, \\ 0, & \text{otherwise,} \end{cases} \tag{4}$$

is the distribution of the vibration velocity at the wedge's bottom, $v_S(r,\varphi)$ describes the vibration velocity of the sound source's points, and S is the sound source's surface. It should be emphasized that, in particular, the distribution of the vibration velocity $v_S(r,\varphi)$ can be discontinuous. Hence, the considered problem can be easily extended to the case when more than one sound source is located at the bottom of the wedge region. For this purpose, it is enough to assume that $v_S(r,\varphi)$ describes the distribution of the vibration velocity for many sound sources, and S denotes their surfaces.

3. Solution of the Helmholtz equation for the acoustic potential

The acoustic potential can be expressed as the following Fourier series (Wright, 2005):

$$\Phi(\mathbf{r}) = \sum_{m=0}^{\infty} \Psi_m(r,z)\cos(\nu_m\,\varphi), \tag{5}$$

where the functions $\Psi_m(r,z)$ are the unknown Fourier coefficients and $\nu_m = m\pi/\varphi_0$. The proposed solution satisfies the boundary conditions given by Eq. (2). Making use of the Hankel transform, the unknown functions from Eq. (5) can be written in the following form (Morse, Ingard, 1968):

$$\Psi_m(r,z) = \int_0^{\infty} J_{\nu_m}(\tau\, r)\chi_m(\tau,z)\tau\,\mathrm{d}\tau, \tag{6}$$

where $J_{\nu_m}(\cdot)$ is the Bessel function of the order ν_m, $\chi_m(\tau, z)$ are the functions to be found. Inserting Eq. (6) into Eq. (5) and using the Helmholtz equation from Eq. (1) result in

$$\frac{\partial^2 \chi_m(\tau, z)}{\partial\, z^2} + \gamma^2 \chi_m(\tau, z) = 0, \tag{7}$$

where $\gamma = \sqrt{k^2 - \tau^2}$. The general solution of the above equation is

$$\chi_m(\tau, z) = A_m(\tau)\, e^{i\gamma\, z} + B_m(\tau) e^{-i\gamma\, z}, \tag{8}$$

where $A_m(\tau)$ and $B_m(\tau)$ are the unknown functions. The first term in Eq. (8) represents outgoing waves, while the second one presents ingoing waves. Taking into account that the sound source is located on the plane $z = 0$, incoming waves cannot be propagated along the z axis and it is necessary to assume that $B_m(\tau) = 0$. Then, combining Eqs. (5), (6), and (8) yields

$$\Phi(\mathbf{r}) = \sum_{m=0}^{\infty} \left(\int_0^{\infty} A_m(\tau) J_{\nu_m}(\tau\, r) e^{i\gamma\, z} \tau\, \mathrm{d}\tau \right) \cos(\nu_m \varphi). \tag{9}$$

The function $A_m(\tau)$ can be found based on the boundary condition from Eq. (3). Using the cosine Fourier series and the Hankel transform of the order ν_m, the distribution of the vibration velocity at the wedge's bottom can be written as follows:

$$v(r, \varphi) = \sum_{m=0}^{\infty} \left(\int_0^{\infty} K_m(\tau) J_{\nu_m}(\tau\, r) \tau\, \mathrm{d}\tau \right) \cos(\nu_m \varphi), \tag{10}$$

where

$$K_m(\tau) = \frac{\varepsilon_m}{\varphi_0} \int_S v_S(r, \varphi) J_{\nu_m}(\tau\, r) \cos(\nu_m \varphi)\, \mathrm{d}S \tag{11}$$

and $\varepsilon_0 = 1$, and $\varepsilon_m = 2$ for $m > 0$. The integration in Eq. (11) is performed over the sound source's surface, which is a consequence of Eq. (4). Inserting Eqs. (9) and (10) into the boundary condition given by Eq. (3) leads to

$$A_m(\tau) = iK_m(\tau)/\gamma. \tag{12}$$

By substituting $\tau = k\vartheta$ into Eq. (9) and using Eq. (12), the acoustic potential can be expressed in the following form:

$$\Phi(\mathbf{r}) = ik \sum_{m=0}^{\infty} \left(\int_0^{\infty} K_m(k\vartheta) J_{\nu_m}(k\vartheta r) e^{ik\mu z} \frac{\vartheta\, \mathrm{d}\vartheta}{\mu} \right) \cdot \cos(\nu_m \varphi), \tag{13}$$

where

$$\mu = \begin{cases} \sqrt{1 - \vartheta^2} & \text{for } \vartheta < 1, \\ i\sqrt{\vartheta^2 - 1} & \text{for } \vartheta > 1. \end{cases} \tag{14}$$

It has been assumed that the argument of μ is equal to 0 when $\vartheta \leq 1$ and it is equal to $\pi/2$ for $\vartheta > 1$. This causes that the integrals appearing in Eq. (13) are convergent and the acoustic potential assumes a finite value at each field point.

4. The sound pressure and sound power

Assuming that the time dependence for the considered processes is given by $\exp(-i\omega t)$, the sound pressure $p(\mathbf{r})$ can be expressed by means of the acoustic potential as follows (cf. Morse, Ingard, 1968; Crocker, 2010):

$$p(\mathbf{r}) = -i\omega\rho\Phi(\mathbf{r}), \tag{15}$$

where ρ is the density of the medium in equilibrium. Inserting Eq. (13) into Eq. (15) results in

$$p(\mathbf{r}) = \frac{\omega^2 \rho}{c} \sum_{m=0}^{M_{\mathrm{ap}}} \left(\int_0^{\infty} K_m(k\vartheta) J_{\nu_m}(k\vartheta\, r) e^{ik\mu\, z} \frac{\vartheta\, \mathrm{d}\vartheta}{\mu} \right) \cdot \cos(\nu_m \varphi). \tag{16}$$

From the practical standpoint, it has been assumed that the upper limit of summation in the above formula is equal to the appropriate finite number M_{ap}. This number should be large enough to achieve a high accuracy of the obtained results. On the basis of the impedance approach, the sound power Π can be formulated as (cf. Pierce, 1981)

$$\Pi = \frac{1}{2} \int_S p(r, \varphi, 0) v_S^*(r, \varphi)\, \mathrm{d}S, \tag{17}$$

where the symbol "*" denotes the conjugate of a complex quantity. Making use of Eqs. (16) and (17), the sound power can be written in the following form:

$$\Pi = \frac{\omega^2 \rho \varphi_0}{2c} \sum_{m=0}^{M_{\mathrm{ap}}} \int_0^{\infty} \frac{K_m(k\vartheta) K_m^*(k\vartheta) \vartheta\, \mathrm{d}\vartheta}{\varepsilon_m \mu}, \tag{18}$$

where

$$K_m^*(\tau) = \frac{\varepsilon_m}{\varphi_0} \int_S v_S^*(r, \varphi) J_{\nu_m}(\tau r) \cos(\nu_m \varphi)\, \mathrm{d}S. \tag{19}$$

The formulas from Eqs. (16) and (18) describe the sound radiation in the case of an arbitrary sound source located at the bottom of the wedge region.

In the case of an arbitrary sound source, the integration over the surface S in Eq. (11) can be performed as follows:

$$K_m(\tau) = \frac{\varepsilon_m}{\varphi_0} \int_{r_{\min}}^{r_{\max}} \int_{\alpha(r)}^{\beta(r)} v_S(r, \varphi) J_{\nu_m}(\tau r) \cdot \cos(\nu_m \varphi)\, \mathrm{d}\varphi r\, \mathrm{d}r, \tag{20}$$

where $r_{\min}$, $r_{\max}$ are the minimal and maximal distance of the source point from the origin of the cylindrical coordinate system, respectively. The functions $\alpha(r)$ and $\beta(r)$ determine the values of the variable φ at the sound source's edges for a fixed value of the variable r. The geometric interpretation of the functions $\alpha(r)$ and $\beta(r)$ has been illustrated in Fig. 2. The integration in Eq. (19) can be performed in an analogous way.

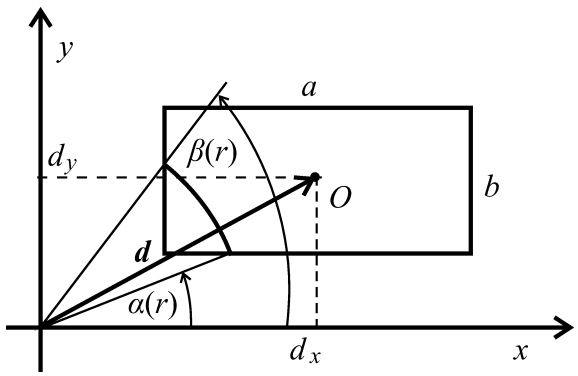

Fig. 2. Piston's location I at the wedge's bottom. The vector $\mathbf{d} = (d_x, d_y)$ indicates the piston's central point. The geometric interpretation of the functions $\alpha(r)$ and $\beta(r)$ appearing in Eq. (20).

In general, the formulas given by Eqs. (16) and (18) contain the triple integrals which can lead to time consuming numerical calculations. If the considered sound source is a piston and $v_S(r,\varphi) = v_0 = \text{const}$, where v_0 denotes the amplitude of the piston's vibration velocity, the formulas from Eqs. (19) and (20) can be rewritten in the form of the following single integral:

$$K_m(\tau) = K_m^*(\tau) = v_0 \int_{r_{\min}}^{r\,\max} U_m(r) J_{\nu_m}(\tau\, r) r \,\mathrm{d}r, \quad (21)$$

where

$$U_m(r) = \begin{cases} (\beta(r) - \alpha(r))/\varphi_0 & \text{for } m = 0, \\ \dfrac{2}{m\pi}\left[\sin\left(\dfrac{m\pi}{\varphi_0}\beta(r)\right) - \sin\left(\dfrac{m\pi}{\varphi_0}\alpha(r)\right)\right] & \text{for } m > 0. \end{cases} \quad (22)$$

On the basis of Eqs. (16), (18), and (21), the sound radiation can be analyzed for a piston of any shape and of an arbitrary location at the wedge's bottom. In the case of this sound source, the formulas describing the sound pressure and sound power can be expressed as a series of double integrals.

5. An example – the sound radiation of a rectangular piston

The obtained formulas given by Eqs. (16) and (18) can be used for many practical applications. In order to show one of them, the sound radiation of a rectangular piston located at the wedge's bottom has been investigated. It has been assumed that the lengths of the piston's sides are equal to $a = 0.2$ m and $b = 0.1$ m. The side of the length a is parallel to the x axis and the location of the piston's central point is defined in the Cartesian coordinate system by the vector $\mathbf{d} = (d_x, d_y)$ (see Fig. 2).

Assuming that $c = 340$ m/s and $\rho = 1.293$ kg/m^3, the analysis has been performed in the case when the wedge region is filled with the air. Moreover, the numerical calculations have been performed for the vibration velocity of the sound source equal to $v_0 = 5 \cdot 10^{-3}$ m/s. The functions $\alpha(r)$ and $\beta(r)$ appearing in Eq. (22) have to be determined for the given piston's location. In the case when the whole surface of the considered sound source lies in the first quadrant of the Cartesian coordinate system, it can be deduced that $\alpha(r) = \alpha_1(r)$ and $\beta(r) = \beta_1(r)$ where

$$\alpha_1(r) = \begin{cases} \arcsin\left(\dfrac{|d_y| - b/2}{r}\right) & \text{for } r_{\min} \le r < r_2, \\ \arccos\left(\dfrac{|d_x| + a/2}{r}\right) & \text{for } r_2 \le r \le r_{\max}, \end{cases} \quad (23)$$

$$\beta_1(r) = \begin{cases} \arccos\left(\dfrac{|d_x| - a/2}{r}\right) & \text{for } r_{\min} \le r < r_1, \\ \arcsin\left(\dfrac{|d_y| + b/2}{r}\right) & \text{for } r_1 \le r \le r_{\max}, \end{cases} \quad (24)$$

where

$$r_{\min} = \sqrt{(|d_x| - a/2)^2 + (|d_y| - b/2)^2},$$

$$r_1 = \sqrt{(|d_x| - a/2)^2 + (|d_y| + b/2)^2},$$

$$r_2 = \sqrt{(|d_x| + a/2)^2 + (|d_y| - b/2)^2},$$

$$r_{\max} = \sqrt{(|d_x| + a/2)^2 + (|d_y| + b/2)^2}.$$

The functions $\alpha(r)$ and $\beta(r)$ can be expressed as $\alpha(r) = \pi - \beta_1(r)$, $\alpha(r) = \pi - \beta_1(r)$ and $\alpha(r) = \pi - \beta_1(r)$, $\beta(r) = \pi + \beta_1(r)$ when the whole piston's surface lies in the second and third quadrant, respectively. The four locations of the piston's central point have been considered: location I – $d_x = 0.25$ m, $d_y = 0.1$ m, location II – $d_x = 0.25$ m, $d_y = 0.25$ m, location III – $d_x = -0.25$ m, $d_y = 0.1$ m and location IV – $d_x = -0.25$ m, $d_y = -0.1$ m. Assuming that the values of the wedge angle are: $\varphi_0 = \pi/3$, $5\pi/6$, $5\pi/4$, $5\pi/3$, the numerical analysis has been performed for the convex as well as concave wedge region. After defining the values of parameters describing the considered vibroacoustic system and determining the functions $\alpha(r)$ and $\beta(r)$ from Eq. (22), the numerical analysis of the sound pressure and power can be performed based on Eqs. (16) and (18).

To find the appropriate value for the upper limit of summation M_{ap} in Eqs. (16) and (18), it is convenient to analyze the following relative error:

$$E_M = \frac{\left|Q_M - Q_M^{(\mathrm{Ref})}\right|}{\left|Q_M^{(\mathrm{Ref})}\right|} 100\%, \tag{25}$$

where Q_M is the value of the quantity Q calculated using all the terms in Eq. (16) or (18) for which $m \leq M$ and $Q_M^{(\mathrm{Ref})}$ is the reference value of the quantity Q calculated by taking into account in Eq. (16) or (18) the number of terms M_{Ref}. The reference value $Q_M^{(\mathrm{Ref})}$ has to be calculated for a large value of the number M_{Ref}. However, M_{Ref} cannot be arbitrarily large to avoid time consuming calculations. Therefore, it has been assumed that $M_{\mathrm{Ref}} = \max(20, 2M)$, where $\max(\eta, \delta)$ is equal to η when $\eta \geq \delta$ and δ if $\eta < \delta$. The number M_{Ref} increases as the number M increases and has a sufficiently large value, even for a small value of the number M. A small value of the relative error E_M means that a contribution of additional terms to the total result is not significant and the series from Eq. (16) and (18) are convergent. Hence, it can be concluded that the obtained results have an acceptable accuracy when the value of E_M is small enough.

In the numerical analysis, it has been assumed that the value of the number M_{ap} appearing in Eqs. (16) and (18) is large enough so that $E_{M_{\mathrm{ap}}} < 1\%$. This leads to obtaining accurate results and formulating correct conclusions.

The formulas from Eqs. (16) and (18) for $\varphi_0 = \pi/2$ represent the generalization of the formulas which can be obtained based on the presented in the literature Green's function valid for the three-wall corner region. Therefore, it is of interest to compare the results obtained by means of the formulas presented in this paper and those obtained on the basis of the Green's function. The formulas describing the sound radiation of the considered piston inside a three-wall corner region obtained by using the Green's function have been presented in Appendix. The validation of the formulas from Eqs. (16) and (18) for $\varphi_0 = \pi/2$ can be performed by estimating the following relative error:

$$E_{\mathrm{com}} = \frac{|Q - Q_{\mathrm{Ref}}|}{Q_{\mathrm{Ref}}} 100\%, \tag{26}$$

where Q is the value calculated from Eq. (16) or Eq. (18), and Q_{Ref} denotes the value determined based on the corresponding formula from Appendix. The formulas obtained by using the Green's function have been considered as correct and exact, while the validity of the present in this paper formulas is investigated.

5.1. Numerical analysis of the sound pressure modulus

On the basis of Eq. (16), the distribution of the sound pressure modulus inside the wedge region can be determined. The values of the sound pressure modulus calculated in the case when $\varphi_0 = \pi/2$ have been compared with the values of this quantity obtained based on Eq. (31). The relative error E_{com} from Eq. (26) has been estimated for the sound pressure modulus at a fixed field point of the coordinate $z = 0.5$ m. It has been assumed that the upper limit of summation in Eq. (16) is equal to $M_{\mathrm{ap}} = 20$. In the case of the piston's location I and the field point located above the central point of the sound source, the relative error E_{com} is equal to about $6 \cdot 10^{-5}\%$ for $f = 0.25$ kHz and about $4 \cdot 10^{-5}\%$ for $f = 0.5$ kHz. When $f = 0.5$ kHz, the quantity E_{com} does not exceed $9 \cdot 10^{-5}\%$ for the piston's location I and the field point $x = 0.5$ m and $y = 0.2$ m. The considered relative error is less than $8 \cdot 10^{-6}\%$ in the case of $f = 0.5$ kHz, the piston's location II and the field point $x = 0.01$ m and $y = 0.25$ m, which is near the transverse baffle. The estimated values of the relative error E_{com} are negligible. Therefore, it can be concluded that in the case of the sound pressure modulus, the results obtained for the wedge region of the angle $\varphi_0 = \pi/2$ agree with the corresponding results obtained on the basis of the Green's function.

In order to determine the value of the upper limit of the summation M_{ap}, the relative error E_M from Eq. (25) has been estimated for the sound pressure modulus in the case of several different field points and some values of the number M. The chosen piston's locations as well as some sample values of the vibration frequency and the wedge angle have been analyzed. In Fig. 3, the sound pressure modulus and the considered relative error have been presented as the functions of the normalized angular coordinate φ/φ_0 for some sample values of the radial coordinate r.

Figure 3a shows that the distribution of the sound pressure modulus is nearly axis-symmetric when the value of the radial coordinate r is sufficiently small, i.e., $r = 0.1$ m. In the vicinity of the baffle given by the equation $\varphi = \varphi_0$, a significant increase in the value of the sound pressure modulus is observed. This fact can be explained by a strong interference of acoustic waves coming directly from the sound source and acoustic waves reflected from the baffle. Figure 3b proves that the maximal value of the relative error E_M estimated within the limits $\varphi \in [0, \varphi_0]$ increases as the value of the radial coordinate r increases. The quantity E_M does not exceed about $10^{-5}\%$ for $r = 0.1$ m, is smaller than 0.1% when $r = 0.5$ m, and does not exceed 1% if $r = 1$ m. This means that the value of the number M_{ap} determined for a maximal analyzed value R of the radial coordinate r can be also used as the value of M_{ap} for all the cases when $r < R$. In Fig. 4, the sound

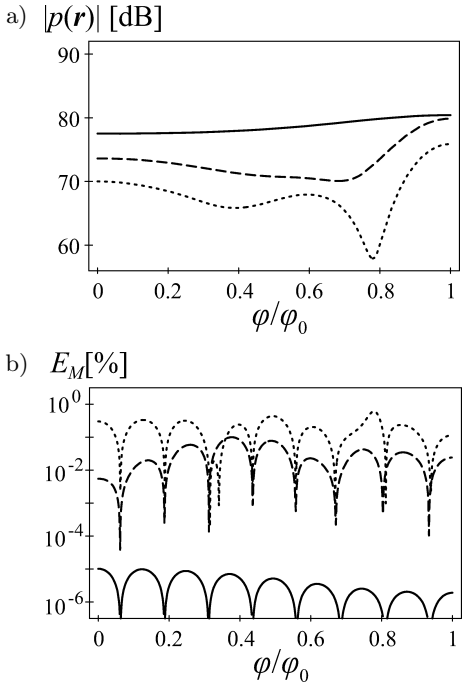

Fig. 3. Sound pressure modulus $|p(\mathbf{r})|$ and the corresponding relative error E_M from Eq. (25) as the functions of the normalized angular coordinate φ/φ_0. It has been assumed that the piston is at location III, $f = 0.5$ kHz, $M = 7$, $z = 0.5$ m, and $\varphi_0 = 5\pi/4$. The line keys: solid – $r = 0.1$ m, dashed – $r = 0.5$ m, dotted – $r = 1$ m.

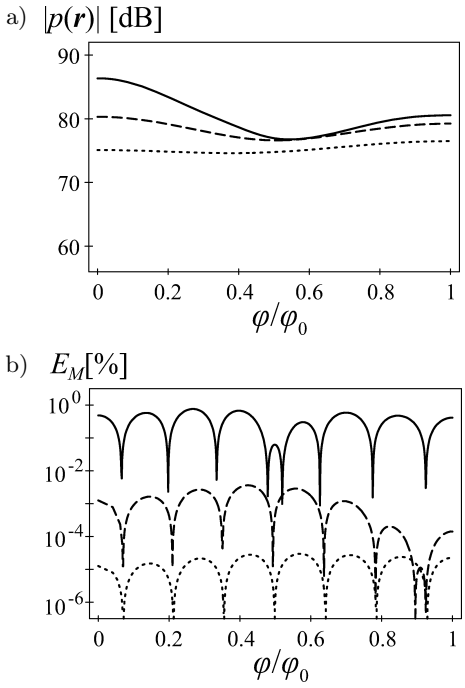

Fig. 4. Sound pressure modulus $|p(\mathbf{r})|$ and the relative error E_M from Eq. (25) as the functions of the normalized angular variable φ/φ_0. The following is assumed: the piston's location I, $f = 0.5$ kHz, $M = 6$, $r = 0.5$ m, and $\varphi_0 = 5\pi/6$. The line keys: solid – $z = 0.1$ m, dashed – $z = 0.5$ m, dotted – $z = 1$ m.

pressure modulus and corresponding relative error E_M have been presented as the functions of the normalized angular coordinate φ/φ_0 for some sample values of the coordinate z.

Based on Fig. 4a, it can be concluded that the increase in the value of the sound pressure modulus is observed in the vicinity of the baffles. Moreover, the increase in the value of the coordinate z causes that the distribution of the sound pressure modulus becomes more similar to the axis-symmetric distribution. The maximal value of the relative error E_M observed within the limits $\varphi \in [0, \varphi_0]$ rapidly diminishes as the value of the coordinate z increases (see Fig. 4b). The value of E_M is smaller than 1% for $z = 0.1$ m and does not exceed 0.01% when $z = 0.5$ m. Therefore, it can be deduced that the value of the upper limit of the summation M_{ap} determined for the minimal analyzed value z_0 of the coordinate z can be used as the value of M_{ap} for all the cases when $z > z_0$. The distribution of the sound pressure modulus on the surface $r \leq 1$ m, $0 \leq \varphi \leq \varphi_0$, and $z = 0.5$ m has been illustrated in Figs. 5–8, while the distribution of this quantity on the surface $0 \leq \varphi \leq \varphi_0$, 0.1 m $\leq z \leq 1$ m, and $r = 0.5$ m has been shown in Fig. 9. The chosen piston's locations and some sample values of the vibration frequency have

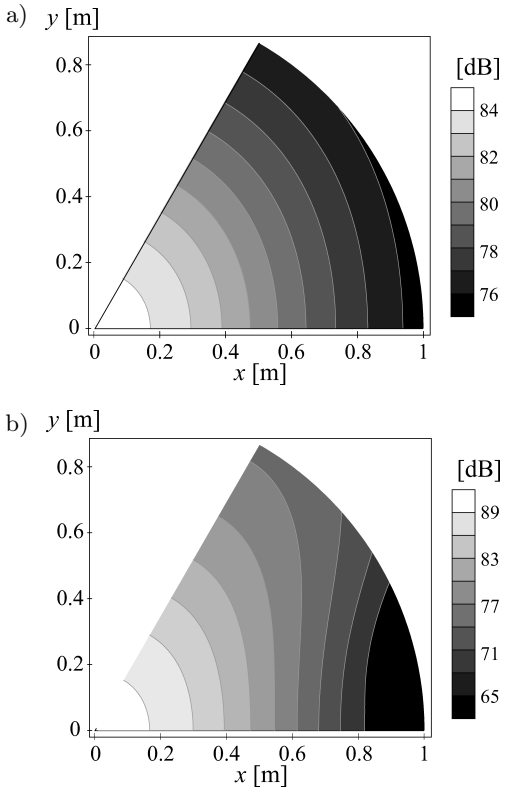

Fig. 5. Distribution of the sound pressure modulus $|p(\mathbf{r})|$ on the surface $r \leq 1$ m, $0 \leq \varphi \leq \varphi_0$, and $z = 0.5$ m for $\varphi_0 = \pi/3$ and the piston's location I. Moreover, the assumptions are such that: a) $f = 0.25$ kHz and $M_{\mathrm{ap}} = 1$, b) $f = 0.5$ kHz and $M_{\mathrm{ap}} = 2$.

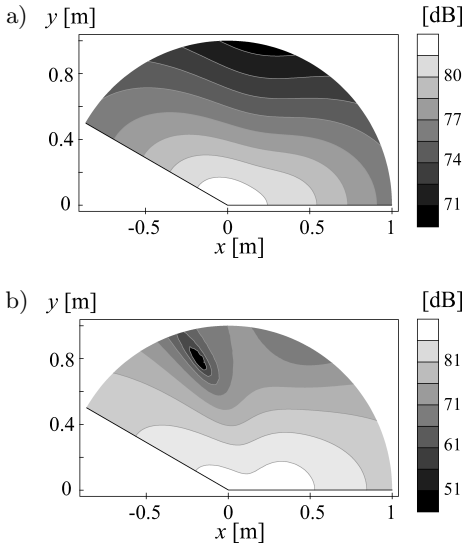

Fig. 6. Distribution of the sound pressure modulus $|p(\mathbf{r})|$ on the surface $r \leq 1$ m, $0 \leq \varphi \leq \varphi_0$ and $z = 0.5$ m for $\varphi_0 = 5\pi/6$ and the piston's location I with the assumption that: a) $f = 0.5$ kHz and $M_{\mathrm{ap}} = 3$ and b) $f = 1$ kHz and $M_{\mathrm{ap}} = 8$.

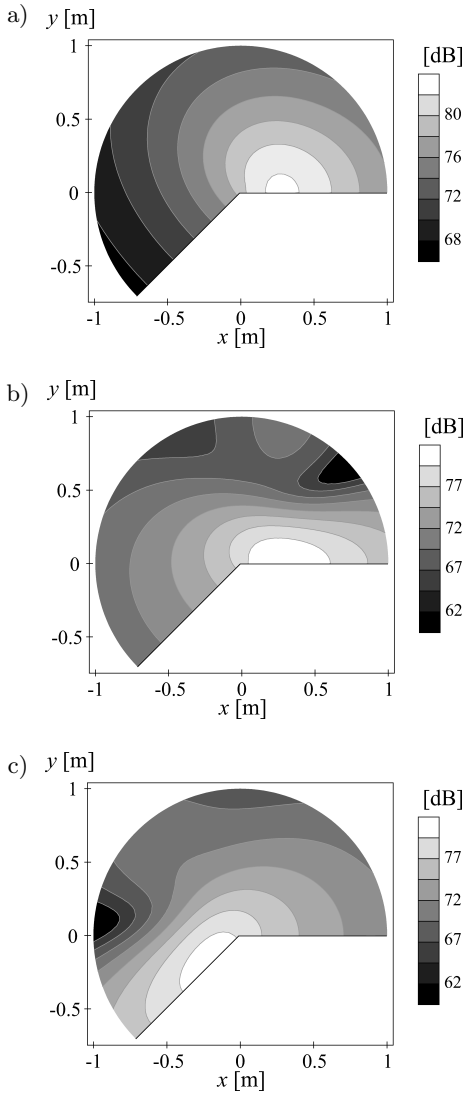

Fig. 7. Distribution of the sound pressure modulus $|p(\mathbf{r})|$ on the surface $r \leq 1$ m, $0 \leq \varphi \leq \varphi_0$ and $z = 0.5$ m for $\varphi_0 = 5\pi/4$, and $f = 0.5$ kHz, with the following assumptions: a) the piston's location I and $M_{\mathrm{ap}} = 5$, b) location II and $M_{\mathrm{ap}} = 9$, c) the piston's location III and $M_{\mathrm{ap}} = 7$.

been investigated. In the case of Figs. 5–8, the upper limit of the summation M_{ap} in Eq. (16) has been assumed as the minimal value of the number M for which the maximal value of the relative error E_M estimated within the limits $\varphi \in [0, \varphi_0]$ and for $r = 1$ m is less than 1%. This causes that $E_{M_{\mathrm{ap}}} < 1\%$ for all the points of the considered surface. In the case of Fig. 9, the number M_{ap} has been estimated so that $E_{M_{\mathrm{ap}}} < 1\%$ for $z = 0.1$ m, $r = 0.5$ m, and within the limits $\varphi \in [0, \varphi_0]$. This allows the quantity $E_{M_{\mathrm{ap}}}$ to be lower than 1% at all the considered points.

The assumed values of M_{ap} have been given in the figures' descriptions. To satisfy the condition $E_{M_{\mathrm{ap}}} < 1\%$ in the case of a small value of the coordinate z, it is necessary to assume a large value for the number M_{ap} This causes that the numerical calculations are very time consuming in the case of the field points located near the plane $z = 0$. Therefore, in Fig. 9, the distribution of the sound pressure modulus has not been illustrated for $z < 0.1$ m. Analyzing the assumed values for the number M_{ap}, it can be noticed that these values increase as the value of the vibration frequency increases. In the case of $\varphi_0 = 5\pi/6$ and the piston's location I, $M_{\mathrm{ap}} = 3$ for $f = 0.5$ kHz and $M_{\mathrm{ap}} = 8$ when $f = 1$ kHz. This effect can be linked to the fact that the distribution of the acoustic field is more complicated for the high vibration frequency.

The increase in the value of the wedge angle causes that the upper limit of the summation M_{ap} increases. For example, in the case of $f = 0.5$ kHz and the piston's location I, $M_{\mathrm{ap}} = 2$ for $\varphi_0 = \pi/3$ and $M_{\mathrm{ap}} = 5$ for $\varphi_0 = 5\pi/4$. This fact can be due to an increase in the surface area of the analyzed acoustic field. Moreover, the value of the number M_{ap} is influenced by the piston's location.

In the case when the wedge region is convex $\varphi_0 = \pi/3,\ 5\pi/6$, the sound pressure modulus assumes some great values for some small values of the radial coordinate r, i.e., in the wedge's corner (see Figs. 5 and 6). Moreover, the distribution of the acoustic field is nearly axis-symmetric if the wedge angle is acute $\varphi_0 = \pi/3$ and the vibration frequency is low $f = 0.25$ kHz (Fig. 5a). The influence of the diffraction of acoustic waves on the distribution of the sound pressure modulus has been illustrated in Figs. 7–9 in the case of the concave wedge region. The distribution of the acoustic

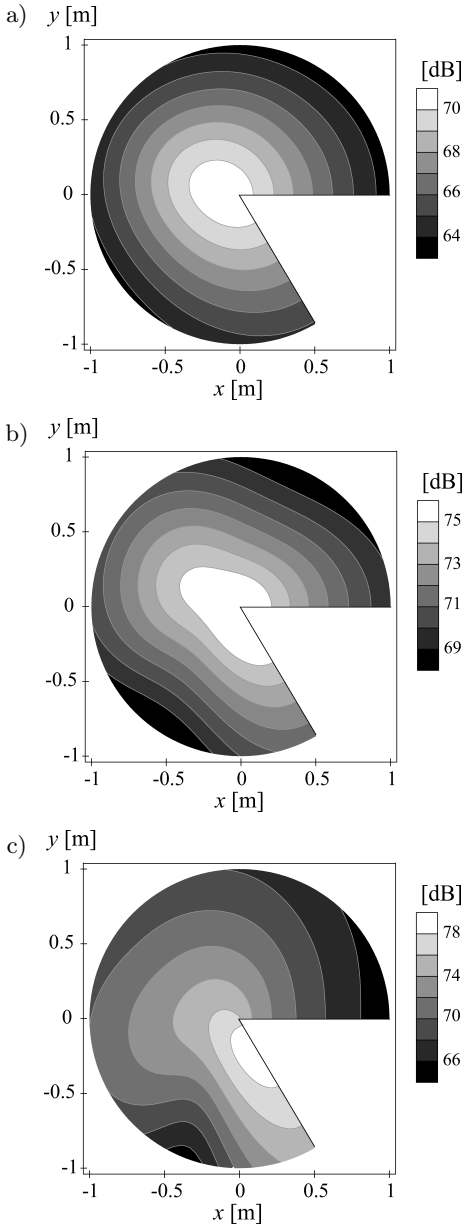

Fig. 8. Distribution of the sound pressure modulus $|p(\mathbf{r})|$ on the surface $r \leq 1$ m, $0 \leq \varphi \leq \varphi_0$, and $z = 0.5$ m for $\varphi_0 = 5\pi/3$. The following has been also assumed: a) $f = 0.25$ kHz, the piston's location III, and $M_{\mathrm{ap}} = 6$, b) $f = 0.5$ Hz, the piston's location III, and $M_{\mathrm{ap}} = 9$, c) $f = 0.5$ kHz, the piston's location IV, and $M_{\mathrm{ap}} = 9$.

field is significantly influenced by the piston's location (see Figs. 7–9). Figure 7 shows that in the case of the piston's location I, some small values of the sound pressure modulus are observed for $\varphi > \pi$ and the values of the coordinate r close to 1 m. This effect is not observed for the piston's locations II and III. Based on Figs. 7, 8c and 9, it can be concluded that the increase in the value of the sound pressure modulus can occur in the vicinity of the transverse baffles.

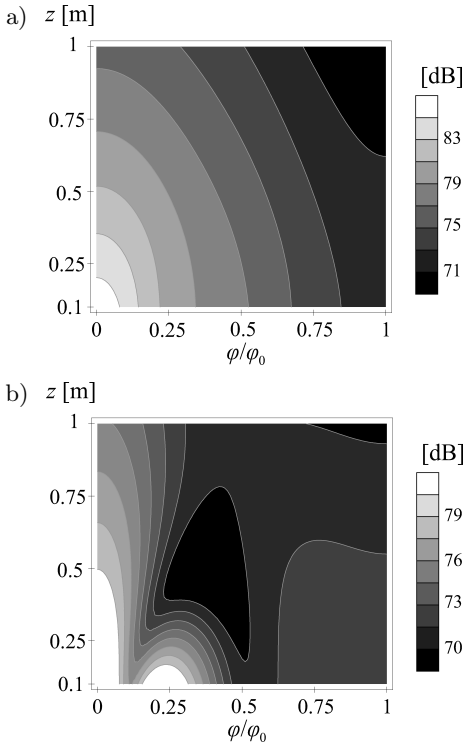

Fig. 9. Distribution of the sound pressure modulus $|p(\mathbf{r})|$ on the surface $0 \leq \varphi \leq \varphi_0$, 0.1 m $\leq z \leq 1$ m and $r = 0.5$ m for $\varphi_0 = 5\pi/4$, and $f = 0.5$ kHz. The following parameters have been also assumed: a) the piston's location I and $M_{\mathrm{ap}} = 9$, b) the piston's location II and $M_{\mathrm{ap}} = 13$.

5.2. Numerical analysis of the sound power

Making use of Eq. (18), the sound power of the considered vibroacoustic system can be calculated. The results obtained from Eq. (18) for $\varphi_0 = \pi/2$ have been compared with the results obtained on the basis of Eq. (33) and valid for the three-wall corner region. The relative error E_{com} given by Eq. (26) has been estimated for the modulus $|\Pi|$ and the phase θ_Π of the sound power. It has been assumed that the upper limit of the summation in Eq. (18) is equal to $M_{\mathrm{ap}} = 50$. The estimated values of the relative error E_{com} show that the calculations performed using Eq. (18) for $\varphi_0 = \pi/2$ and Eq. (33) lead to very similar results. For example, in the case of the following values of the vibration frequency: $f = 0.5$ kHz, 1 kHz and 1.5 kHz, the quantity E_{com} calculated for the sound power modulus does not exceed 0.1% and 0.13% for the piston's location I and the piston's location II, respectively. This relative error calculated for the sound power phase and the same values of the vibration frequency is lower than 0.02% in the case of the piston's location I and II. It can be noticed that the relative error E_{com} assumes much smaller values in the case of the modulus than in the case of the phase of the sound power. The small dif-

ferences between the results obtained from Eq. (18) and Eq. (33) can be due to assuming the finite upper limit of the summation in Eq. (18) as well as to some numerical procedures. Therefore, it can be concluded that these results agree with each other. In Figs. 10 and 11, the modulus and phase of the sound power have been presented as the functions of the vibration frequency for some sample values of the wedge angle and for some chosen piston's locations.

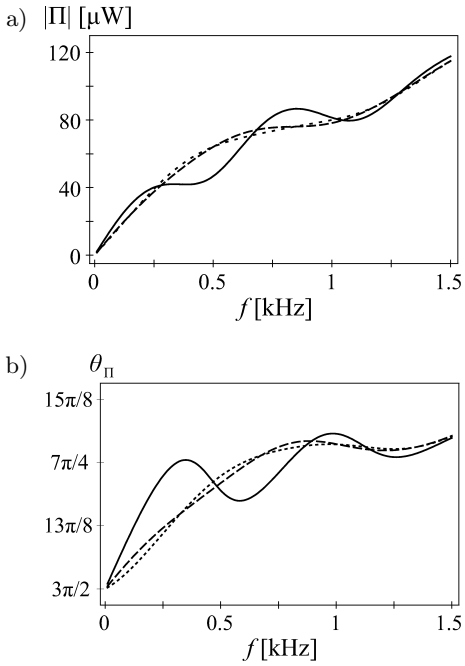

Fig. 10. Sound power: a) modulus $|\Pi|$, b) phase θ_Π as the functions of the vibration frequency for the piston's location I. The line keys: solid – $\varphi_0 = \pi/3$ and $M_{\mathrm{ap}} = 7$, dashed – $\varphi_0 = 5\pi/6$ and $M_{\mathrm{ap}} = 10$, and dotted – $\varphi_0 = 2\pi$ and $M_{\mathrm{ap}} = 25$.

In order to determine the value for the upper limit of summation M_{ap} in Eq. (18), the relative error E_M from Eq. (25) has been estimated for the modulus and phase of the sound power. The value of the number M_{ap} has been assumed so that $E_{M_{\mathrm{ap}}} < 1\%$ for all the analyzed cases and it has been given in the figures' descriptions. It is worth noting that the value of M_{ap} increases as the value of the wedge angle does. Moreover, the value of M_{ap} is influenced by the piston's location. To illustrate the behaviour of the relative error $E_{M_{\mathrm{ap}}}$, this quantity calculated for the modulus as well as the phase of the sound power has been presented in Fig. 12 as a function of the vibration frequency in some selected cases.

The relative error $E_{M_{\mathrm{ap}}}$ has been estimated for the following values of the vibration frequency $f = 50n$ Hz where n is an integer and $1 \leq n \leq 30$. Figure 12 confirms that in the case of the modulus as well as the phase of the sound power, the value of $E_{M_{\mathrm{ap}}}$ is smaller

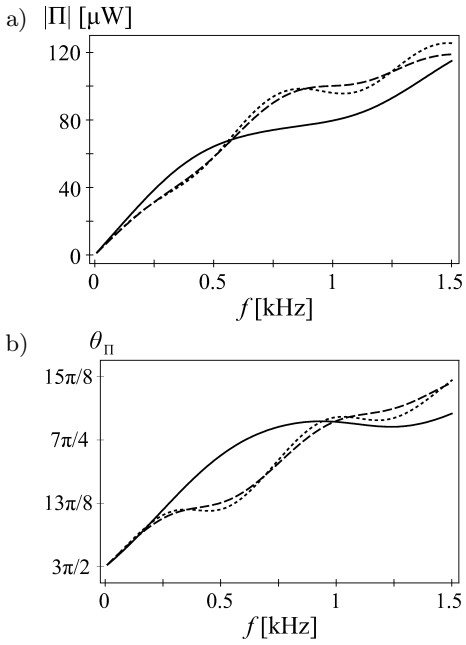

Fig. 11. Sound power: a) modulus $|\Pi|$, b) phase θ_Π as the functions of the vibration frequency for $\varphi_0 = 5\pi/4$. The line keys: solid – the piston's location I and $M_{\mathrm{ap}} = 16$, dashed – the piston's location II and $M_{\mathrm{ap}} = 28$, and dotted – the piston's location III and $M_{\mathrm{ap}} = 18$.

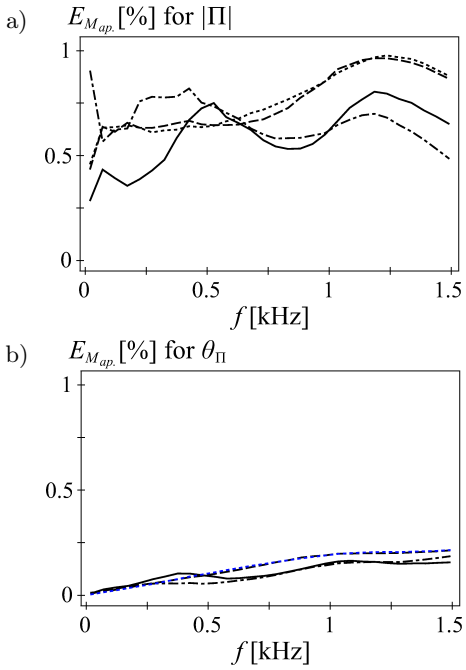

Fig. 12. Relative error E_M given by Eq. (25) calculated for: a) the sound power modulus $|\Pi|$, b) the sound power phase θ_Π as the functions of the vibration frequency. The line keys: solid – $\varphi_0 = \pi/3$, $M_{\mathrm{ap}} = 7$ and the piston's location I, dashed – $\varphi_0 = 5\pi/6$, $M_{\mathrm{ap}} = 10$ and the piston's location I, dashed-dotted – $\varphi_0 = 5\pi/4$, $M_{\mathrm{ap}} = 28$ and the piston's location II, and dotted – $\varphi_0 = 2\pi$, $M_{\mathrm{ap}} = 25$ and the piston's location I.

than 1% for all the analyzed values of the vibration frequency. Moreover, it can be noticed that the quantity $E_{M_{\rm ap}}$ assumes some greater values for the sound power modulus than for the sound power phase.

In Fig. 10, the curves obtained for $\varphi_0 = \pi$, $5\pi/4$ and $5\pi/3$ lie very close to the curve obtained in the case of $\varphi_0 = 2\pi$. Therefore, taking into account the figures' clarity, these curves have not been presented. Figure 10 shows that the increase in the value of the wedge angle from $\varphi_0 = \pi/3$ to $\varphi_0 = 5\pi/6$ causes a considerable change in both the modulus and phase of the sound power. This effect can be due to a significant change in the interference of acoustic waves reflected from the transverse baffles. Moreover, the sound power is slightly influenced by the value of the wedge angle when $\varphi_0 > \pi/2$.

Figure 11 illustrates the influence of the piston's location on the sound power. It can be concluded that a change in the piston's location causes a significant change in both the modulus and phase of the sound power when the value of the vibration frequency is greater than about 0.25 kHz. However, the sound power is not considerably influenced by the piston's location when the value of the vibration frequency is lower than about 0.2 kHz.

From the practical standpoint, it is of interest to investigate the influence of the transverse baffles on the sound power. This influence has been analyzed in the case of the baffle given by the equation $\varphi = \varphi_0$. For this purpose, the following normalized quantities have been introduced:

$$q_m = |\Pi| / \Pi_m^{(\mathrm{Ref})}, \qquad q_p = \theta_\Pi / \theta_\Pi^{(\mathrm{Ref})}, \qquad (27)$$

where $\Pi_m^{(\mathrm{Ref})}$ and $\theta_\Pi^{(\mathrm{Ref})}$ denote the modulus and the phase of the reference sound power, respectively. The reference sound power has been calculated for $M_{\rm ap} = 25$ and in the case when the baffle of the equation $\varphi = \varphi_0$ is absent, i.e., when $\varphi_0 = 2\pi$. Moreover, it has been assumed that all the quantities appearing in Eq. (27) have been calculated for the piston's location I. The quantities q_m and q_p have been presented in Fig. 13 as the functions of the vibration frequency for some sample values of the wedge angle.

Figure 13 shows that the influence of the considered baffle on the modulus and phase of the sound power decreases as the value of the vibration frequency increases. This effect can be explained by the fact that the sound radiation of a source becomes more focused in the direction perpendicular to its surface when the value of the vibration frequency increases, which is the cause of diminishing of the influence of acoustic waves reflected from the baffle on the sound power. Based on Fig. 13, it can be noticed that the considered baffle has a greater influence on the sound power modulus than on the sound power phase. Moreover, it can be also concluded that the analyzed influence decreases as the value of the wedge angle increases.

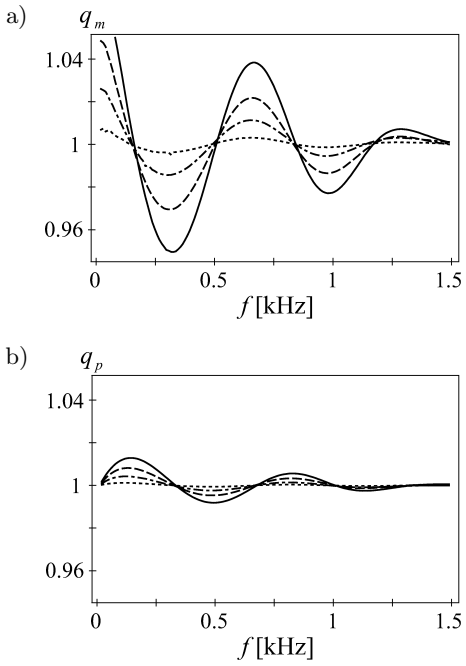

Fig. 13. Quantities: a) q_m, b) q_p given by Eq. (27) as the functions of the vibration frequency. It has been assumed that the modulus $|\Pi|$ and phase θ_Π of the sound power appearing in Eq. (27) have been calculated for: solid line – $\varphi_0 = 5\pi/6$ and $M_{\rm ap} = 10$, dashed line – $\varphi_0 = \pi$ and $M_{\rm ap} = 12$, dashed-dotted line – $\varphi_0 = 5\pi/4$ and $M_{\rm ap} = 16$, and dotted line – $\varphi_0 = 5\pi/3$ and $M_{\rm ap} = 21$.

This is due to the fact that the influence of reflected and diffracted waves on the sound power diminishes as the value of the wedge angle increases. Making use of Fig. 13, the minimal value of the vibration frequency, for which the influence of the considered baffle on the sound power can be ignored with a small value of error, can be determined. For example, without taking into account the influence of the considered baffle on the sound power, some accurate results can be obtained when $f > 1.15$ kHz and $\varphi_0 > 5\pi/6$. In particular, the performed numerical analysis confirms that the semi-infinite transverse baffle can be modelled by the infinite baffle when the value of the vibration frequency is sufficiently high.

6. Conclusions

The formulas describing the sound radiation inside the wedge region bounded by perfectly rigid and infinite baffles have been obtained. They are valid for any value of the wedge angle and represent a generalization of the formulas describing the sound radiation inside the two or three wall corner regions. Moreover, these analytical formulations can be easily extended to the case when more than one sound source is located at the wedge's bottom, which increases their applicability.

As an illustrative example of a practical application, the obtained formulas have been used to investigate the sound radiation of the rectangular piston located at the bottom of the wedge region. The distribution of the sound pressure modulus inside the considered region has been analyzed. The performed numerical calculations show that in the case of the convex wedge region, large values of the sound pressure modulus occur in the wedge's corner. It can be also concluded that the distribution of the acoustic field is nearly axis-symmetric when the wedge angle is acute and the value of the vibration frequency is small. As expected, the theoretical investigations confirm the increase in the value of the sound pressure modulus in the vicinity of the transverse baffles. Moreover, they predict a strong influence of the sound source's location on the distribution of the acoustic field.

On the basis of the obtained formulas, the sound power has been investigated in the case of the values of the vibration frequency smaller than 1.5 kHz. Some sample values of the wedge angle as well as some selected piston's locations have been analyzed. The influence of the transverse baffle on the sound power has been discussed. The numerical analysis shows that this influence decreases as the value of the vibration frequency increases. It has also been proved by the numerical calculations that in the case of the sound power, the semi-infinite transverse baffle can be modelled by the infinite baffle when the value of the vibration frequency is sufficiently high. This fact can be used to simplify some theoretical investigations.

The performed numerical analysis shows that the obtained formulas allow for predicting of the acoustic behaviour of the considered vibroacoustic system. Hence, it can be concluded that they can be used, in the future, for both noise control and many other practical applications.

Appendix. Formulas describing the sound radiation of a rectangular piston inside the three-wall corner region obtained by using the Green's function

In the study (Rdzanek, Rdzanek, 2006), the Green's function for the three-wall corner region has been presented in the following form:

$$G\left(\mathbf{r}|\mathbf{r}_S\right) = \frac{4ik^2}{\pi^2}\int\limits_0^{\infty}\int\limits_0^{\pi/2}\cos(\xi\, x)\cos(\xi\, x_S) \cdot \cos(\eta\, y)\cos(\eta\, y_S)e^{i\gamma\, z}\frac{\tau\,\mathrm{d}\tau\,\mathrm{d}\theta}{\gamma}, \quad (28)$$

where $\xi = k\tau\cos\theta$, $\eta = k\tau\sin\theta$ and

$$\gamma = \begin{cases} k\sqrt{1-\tau^2} & \text{for } 0<\tau<1, \\ ik\sqrt{\tau^2-1} & \text{for } \tau>1, \end{cases} \quad (29)$$

are the components of the wave vector $\mathbf{k}$ in the Cartesian coordinate system, $\mathbf{r} = (x, y, z)$ denotes the vector defining the location of field point P, and $\mathbf{r}_S = (x_s, y_S)$ is the vector determining the location of sound source's point G on the plane $z = 0$ (see Fig. 14).

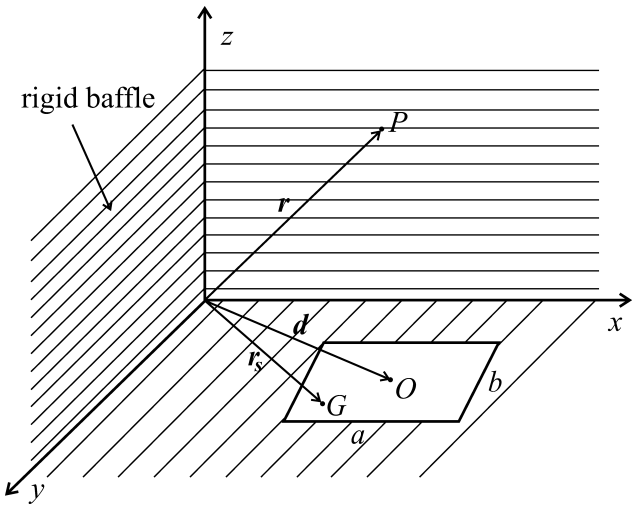

Fig. 14. Considered sound source at the boundary of the three-wall corner region. The introduced Cartesian coordinate system and the vectors $\mathbf{r}$ and $\mathbf{r}_s$ determining the locations of the field point and source point, respectively.

Based on this function, the formulas describing the sound radiation can be obtained in particular cases, i.e., when the sound source is located at the bottom of the wedge region with the angle $\varphi_0 = \pi/2$.

The sound pressure can be expressed with the aid of the Green's function as follows:

$$p(\mathbf{r}) = -i\omega\rho\int\limits_S v_S(\mathbf{r}_S)G(\mathbf{r}|\mathbf{r}_S)\,\mathrm{d}S, \quad (30)$$

where $v_S(\mathbf{r}_S)$ is the vibration velocity of the sound source's points and S denotes the sound source's surface.

It has been assumed that the sound source is a rectangular piston with the sides equal to a and b, and the location of the central point given by the vector $\mathbf{d} = (d_x, d_y)$. The piston's location has been shown in Fig. 14. In the case of the considered sound source, the sound pressure from Eq. (30) can be written in the following form:

$$p(\mathbf{r}) = \frac{4\omega\rho v_0 k^2}{\pi^2}\int\limits_0^{\infty}\int\limits_0^{\pi/2}M(\tau,\theta)\cos(\xi\, x) \cdot \cos(\eta y)e^{i\gamma z}\frac{\tau\,\mathrm{d}\tau\,\mathrm{d}\theta}{\gamma}, \quad (31)$$

where

$$M(\tau,\theta)=\frac{4}{\xi\eta}\sin\left(\xi\frac{a}{2}\right)\cos(\xi d_x)\sin\left(\eta\frac{b}{2}\right)\cos(\eta d_y). \quad (32)$$

Then, making use of the impedance approach and Eq. (31), the formula for the sound power can be presented as

$$\Pi = \frac{1}{2}\int_S p(x,y,0)v_S^*(\mathbf{r}_S)\,\mathrm{d}S$$

$$= \frac{2\omega\rho v_0^2k^2}{\pi^2}\int_0^{\infty}\int_0^{\pi/2} M^2(\tau,\theta)\frac{\tau\,\mathrm{d}\tau\,\mathrm{d}\theta}{\gamma}. \quad (33)$$

The results obtained based on Eqs. (31) and (33) have been compared with the corresponding results obtained for the wedge region of the angle $\varphi_0=\pi/2$.

Acknowledgment

The research for this paper was partially financially supported by the Project of the Centre of Innovation and Knowledge Transfer of Technical and Natural Sciences at the University of Rzeszów.

References

1. Abawi A.T., Porter M.B. (2007), *Propagation in an elastic wedge using the virtual source technique*, The Journal of the Acoustical Society of America, **121**, 3, 1374–1382.
2. Aretz M., Dietrich P., Vorländer M. (2014), *Application of the mirror source method for low frequency sound prediction in rectangular rooms*, Acta Acustica united with Acustica, **100**, 2, 306–319.
3. Budaev B.V., Bogy D.B. (2003), *Random walk approach to wave propagation in wedges and cones*, The Journal of the Acoustical Society of America, **114**, 4, 1733–1741.
4. Crocker M.J. (2010), *Handbook of acoustics*, Wiley, New York.
5. Godinho L., Branco F.G., Mendes P.A. (2011), *3D multi-domain MFS analysis of sound pressure level reduction between connected enclosures*, Archives of Acoustics, **36**, 3, 575–601.
6. González-Montenegro M.A., Jordan R., Lenzi A., Arenas J.P. (2014), *A numerical approach to calculate the radiation efficiency of baffled planar structures using the far field*, Archives of Acoustics, **39**, 2, 249–260.
7. Górski P., Morzyński L. (2013), *Active noise reduction algorithm based on notch filter and genetic algorithm*, Archives of Acoustics, **38**, 2, 185–190.
8. Hasheminejad S.M., Azarpeyvand M. (2004), *Sound radiation due to modal vibrations of a spherical source in an acoustic quarterspace*, Shock and Vibration, **11**, 625–635.
9. Hladky-Hennion A.-C., Langlet P., Bossut R., de Billy M. (1998), *Finite element modelling of radiating waves in immersed wedges*, Journal of Sound and Vibration, **212**, 2, 265–274.
10. Leniowska L. (2009), *Modelling and vibration control of planar systems by the use of piezoelectric actuators*, Archives of Acoustics, **34**, 4, 507–519.
11. Mazur K., Pawełczyk M. (2013), *Active noise control with a single nonlinear control filter for a vibrating plate with multiple actuators*, Archives of Acoustics, **38**, 4, 537–545.
12. Mechel F. (2013), *Room acoustical fields*, Springer-Verlag, Berlin, Heidelberg.
13. Meissner M. (2013), *Evaluation of decay times from noisy room responses with pure-tone excitation*, Archives of Acoustics, **38**, 1, 47–54.
14. Morse P.M., Ingard K.U. (1968), *Theoretical acoustics*, McGraw-Hill, Inc., Princeton, New Jersey.
15. Palumbo D. (2009), *Estimating sound power radiated from rectangular baffled panels using a radiation factor*, The Journal of the Acoustical Society of America, **126**, 4, 1827–1837.
16. Pierce A.D. (1981), *Acoustics: an introduction to its physical principles and applications*, McGraw-Hill Book Co., New York.
17. Rdzanek W.J., Rdzanek W.P. (2006), *Green function for the problem of sound radiation by a circular sound source located near two-wall corner and three-wall corner*, Archives of Acoustics, **31**, 4 (Supplement), 99–106.
18. Rdzanek W.P., Szemela K., Pieczonka D. (2007), *Sound pressure radiation of a circular piston located at a two- and three-wall corners*, Archives of Acoustics, **32**, 4, 883–893.
19. Szemela K. (2014), *The sound radiation of a vibrating baffled simply supported rectangular plate located near two flat transverse baffles*, Acta Acustica united with Acustica, **100**, 4, 604–613.
20. Szemela K., Rdzanek W.P., Rdzanek W.J. (2012), *Acoustic power radiated by a system of two vibrating circular membranes located at the boundary of three-wall corner spatial region*, Archives of Acoustics, **37**, 4, 463–473.
21. Wiciak M., Trojanowski R. (2013), *Modeling of a circular plate with piezoelectric actuators of arbitrary shape*, Acta Physica Polonica A, **123**, 6, 1048–1053.
22. Wright M.C.M. (2005), *Lecture notes on the mathematics of acoustics*, Imperial College Press, London.